UHF RiverSonde Streamflow Measurements at the Cowlitz River: Final Report

Calvin C. Teague, Donald E. Barrick and Peter M. Lilleboe
CODAR Ocean Sensors, Ltd.
1914 Plymouth Street
Mountain View, CA 94043
(408) 773-8240
cal@alpha.stanford.edu, don@codaros.com, pete@codaros.com

April 15, 2005

Abstract

An extended field experiment was conducted from October 2003 through June 2004 using a CODAR RiverSonde UHF radar system at Castle Rock, Washington, USA on the Cowlitz River. A monostatic radar configuration on one bank of the river, with the antennas looking both upriver and downriver, provided high-quality data. Estimates of the along-channel velocity were made using least-squares fits of radial flow velocities in 5-m wide strips across the channel. The surface velocity typically was about 1.0 m/s, but it reached nearly 3.5 m/s on 30 January 2004. Hourly means of the cross-channel profile were calculated for the entire experiment and were used to create a multi-month time series of mean velocity. The velocity time series was combined with a ground-penetrating radar measurement of the bottom profile and stage height to provide a time series of volume discharge.

In addition to the UHF RiverSonde instrumentation, a weather station was installed in December 2003 and recorded wind, temperature, humidity and rainfall every ten minutes, and a video camera (a "webcam") periodically recorded images of the river and surrounding area. Also, several microwave radar systems operated by the University of Washington were in operation within about 100 m of the UHF system.

The radar velocity time series agreed very well with the *in-situ* stage height measurements made by the USGS at a location about 130 m downstream of the radar location, and the volume discharge estimated from the radar velocity measurements agreed very well with the volume discharge estimated by the USGS using the stage height rating curve for the Cowlitz site. The cross-channel velocity profiles were compared with *in-situ* USGS acoustic measurements made from a tethered platform about 50 m upstream of the radar and from a bridge about 100 m downstream of the radar. The radar velocity profiles agreed well with the acoustic profiles in the middle of the channel, although the radar did not see the decrease in velocity at the two banks as observed by the acoustic instruments. This may have been due to shadowing of the radar energy by the bank between the radar antenna and the water at the near shore, and by limited coverage of along-channel velocity vectors at the far shore. The volume discharge estimated from the RiverSonde measurements tracked the USGS volume estimates with an R^2 value of 0.98 when using the *in-situ* stage height measurements and 0.95 when the stage height was estimated from the RiverSonde velocity data. Finally, a small periodic diurnal signal was apparent in the radar data but very weak in the stage data. The periodic signal was well modeled by several tidal frequencies, with the diurnal and semidiurnal terms dominating. Tidal influence on the velocity signal at Castle Rock is plausible given the strong tidal signal seen at the Columbia River at Longview, Washington. The RiverSonde measurements agreed very well with the microwave measurements, including the periodic tidal signal. The wind appeared to have very little influence on the velocity measurements.

Introduction

Recently there has been interest in non-contact methods of measuring river streamflow. One approach, discussed here, is to use ultra-high frequency (UHF) radar, mounted on the bank of a river or on a bridge or other structure, to measure the river surface velocity remotely. For several decades, high-frequency (HF) radar, using wavelengths of several tens of meters, has been used routinely to measure ocean surface currents [*Barrick*, 1971]. Recently, one of these systems, SeaSonde®, has been extended to operate at UHF, using a radar wavelength of approximately 1 m.

HF and UHF radar systems measure radial surface velocity by exploiting the Bragg scattering phenomenon. When observing a water surface, the strongest signals observed by the radar are generated by first-order scattering from the Bragg waves which are traveling radially toward or away from the radar and which have a wavelength equal to one-half the radar wavelength [*Crombie*, 1955]. (Scattering from other water waves occurs, but the reflected energy is not directed toward the radar.) In deep water (with a depth of at least one-quarter of the water wavelength), these waves have a phase velocity given by $v_p = \sqrt{gL/2\pi}$, where g is the gravitational acceleration and L is the water wavelength (equal to one-half the radar wavelength λ). Since the radar wavelength is known, the water wavelength and the Doppler shift $f_p = 2v_p/\lambda$ due to the water phase velocity also are known. The waves are advected by a mean flow velocity v_w, which produces an additional Doppler shift of $f_w = (2v_w/\lambda)\cos\theta$, where θ is the angle between the flow direction and the radar look direction. The total Doppler shift observed by the radar is just $f_t = f_p + f_w$ [*Barrick et al.*, 1974]. By measuring f_t and θ, and knowing f_p, it is possible to determine $v_w \cos\theta$. The radar makes three basic measurements: the Doppler frequency f_t, the distance or range r to the scattering patch, and the direction of arrival θ of the radar echoes. From these, the radial component of the flow velocity can be mapped as a function of position on the water surface. If, in addition, the flow is assumed to be predominantly in one direction, as is often the case for a river, the total flow velocity and the cross-channel flow profile can be estimated.

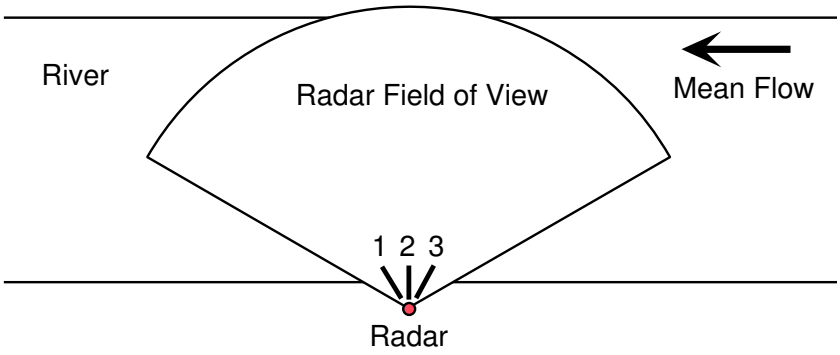

Figure 1: Typical monostatic radar configuration. Antennas 1, 2 and 3 look broadly across the mean direction of flow from a location on the bank.

Previous Experiments

The RiverSonde has been used in a number of short experiments, each lasting only a day or two. Initial tests were done on the American River [*Teague et al.*, 2001] and on the Delta Mendota Canal in California [*Teague et al.*, 2002], using a bistatic radar configuration with transmitting and receiving antennas on opposite sides of the water channel. Subsequent experiments on the Delta Mendota Canal and at Vernalis, California [*Teague et al.*, 2002, 2003] made use of a monostatic geometry with the transmitting and receiving antennas at the same location, either on the bank looking broadly across the direction of flow, or on a bridge looking into the flow direction. Although a location on a bridge might seem attractive, it does not appear to work as well as a location on a bank, because the frequency of the radar signal is broadened when looking across the flow, and the direction-finding procedure works better when signals from different directions arrive at significantly different Doppler frequencies. Consequently, a location on a bank generally is preferred. A typical configuration is shown in Fig. 1.

Cowlitz River Experiment

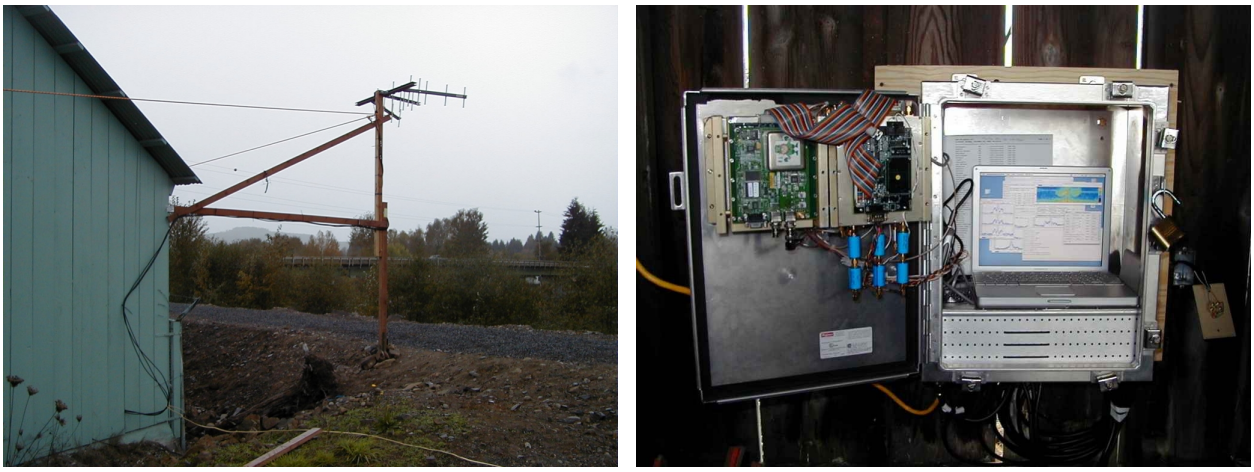

Figure 2: (a) RiverSonde antenna. Energy was transmitted on the center yagi and received on all 3 yagis. (b) RiverSonde equipment and laptop computer. The weather-resistant enclosure was installed inside the storage building seen at the left in (a).

In order to evaluate the performance of a radar river flow measurement system, an experiment was started on 28 October 2003 and was continued until 30 June 2004. The location was on the Cowlitz River at Castle Rock, Washington, USA, about 28 km from the confluence of the Cowlitz and Columbia Rivers, which is about 86 km from the west coast of Washington at the Pacific Ocean. The U. S. Geological Survey maintains a river gaging station at Castle Rock which provides stage height measurements every 15 minutes. In addition, on several occasions, the Geological Survey deployed several *in-situ* instruments to measure water depth using a ground-penetrating radar,

and the vertical and horizontal profiles of velocity using several acoustic instruments. Finally, two microwave radar systems were installed by the University of Washington at the same site. After the experiment was started, a weather station was added to the suite of instruments. The weather station recorded wind speed and direction, air temperature, barometric pressure, rainfall and humidity. Data from all of these systems were available for analysis.

The RiverSonde system was installed in a shelter on one side of the river, with the antenna about 30 m from the near bank looking directly across the river. The river is about 88 m wide, with the far bank about 118 m from the antenna. The water depth was about 3 m at the start of the experiment. Radar data were recorded continuously and processed in hourly blocks on-site on a Macintosh laptop computer. Data were recorded to a local disk, and a dial-up modem provided remote access to both the data and the controlling programs. The weather data were recorded every ten minutes. The radar antenna system consisted of three multi-element yagis, separated by one-half of the radar wavelength and oriented in different directions, with the outer yagis rotated 30° from the direction of the center antenna. This antenna configuration allows the direction of arrival of the radar echoes to be measured to a resolution of about 1° using MUSIC direction finding [*Schmidt*, 1986]. The range resolution of the radar was set to 5 m, with a maximum range of 140 m. Transmitted power was less than 1 W. The antenna is shown in Fig. 2a and the radar equipment and computer are shown in Fig. 2b.

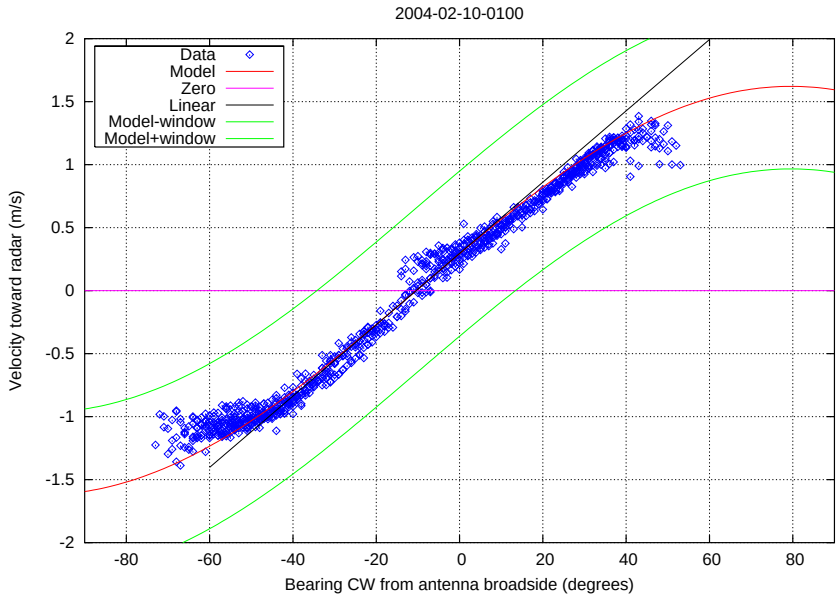

Figure 3: Radial velocity at all ranges *vs* arrival direction. The perpendicular to the mean flow direction is estimated from the zero-crossing of a linear fit to the data, and the slope of the linear fit gives a rough estimate of the magnitude of the velocity.

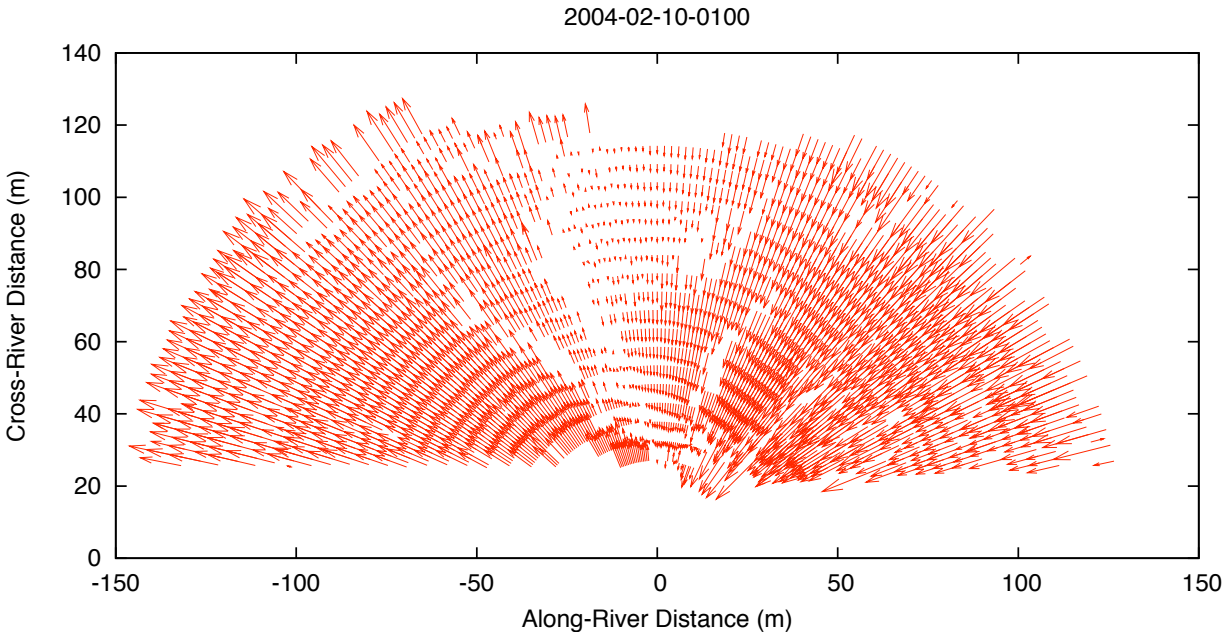

Figure 4: Radial flow vectors averaged over one hour on 10 February 2004. Vectors are plotted between the river banks with 1° resolution in angle and 5 m in range. A velocity of 1.0 m/s is plotted with an equivalent length of 10 m.

Data Processing

Radar data were processed in blocks covering about 2.5 minutes each. Radar returns were first separated into 5 m range bins, and within each range bin, data were separated into separate frequency bins using conventional Fourier transforms. At each range bin and frequency bin, the direction of arrival of one or two signals was determined using the MUSIC algorithm [*Schmidt*, 1986]. Based on a rough estimate of the mean water velocity, the velocity of the Bragg waves either approaching or receding from the radar was subtracted, leaving an estimate of the radial water velocity. For each Doppler shift and arrival angle, if the total Doppler shift was greater than that expected from the estimated velocity projected onto the arrival direction, the approaching wave velocity was used; otherwise the receding wave velocity was used. The estimates were taken from the data processed during the previous hour, or zero if no previous estimates were available. This procedure allows recovery of velocity estimates even for cases in which the spectra of the approaching and receding energy overlap, because overlapping signals usually arrive from different directions (upstream or downstream). As a check, the estimated radial velocity after subtracting the velocity of the approaching or receding waves is plotted against arrival direction. An example is shown in Fig. 3. For a uniform cross-channel profile, the points should follow a sine curve whose amplitude and slope at the zero crossing are linearly related to the velocity, and the angle of zero crossing gives the direction perpendicular to the mean flow direction. In Fig. 3, this direction is approximately 8° counter-clockwise from the antenna broadside direction. (The mean flow direction was not exactly perpendicular to the center of the antenna beam because the antenna orientation was estimated vi-

sually at the antenna location, which was about 30 m from the near bank.) The velocity estimated from the slope provides a surprisingly good estimate of the mean velocity, but gives no information about cross-channel variation.

From the radial velocity estimates, a table of water velocity, distance from the radar, and angle of arrival was constructed. This procedure was repeated for 20 blocks of data covering about an hour. The results were averaged over the hour, and at each range bin a median filter was applied over 5 adjacent angle bins to detect and discard extraneous velocity estimates due to noise or echoes from passing boats. A map of radial velocity vectors was constructed from the averaged and filtered data; an example is shown in Fig. 4. About 15,000 individual vectors were used to compute the averages shown.

Once the smoothed radial vectors were available, the cross-channel velocity profile was estimated using two different techniques. In the first method, similar to the technique used with the narrow-beam microwave system, averages of radial velocity estimates in 5°-wide sectors centered $\pm 15, 20, \ldots, 45°$ from the perpendicular to the estimated flow direction were combined to estimate the along-channel component of velocity. An example of the cross-channel velocity profile using this technique is shown in Fig. 5a. The symbols represent the means of the estimates at each pair of angles over the 20 segments, and the error bars represent the standard deviation of the 20 estimates.

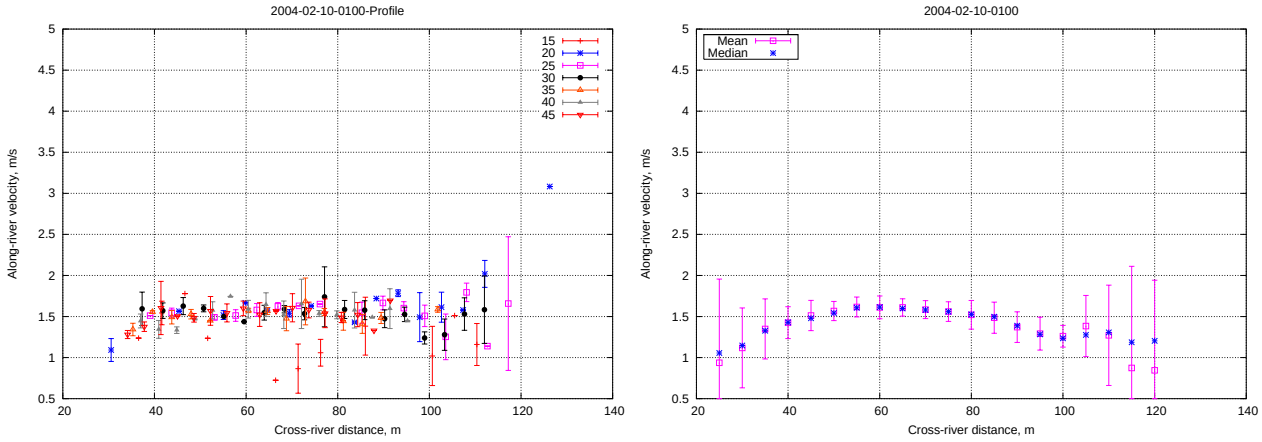

Figure 5: (a) Cross-channel velocity profile estimated from radial vectors $\pm 15, 20, \ldots, 45°$ from the perpendicular to the estimated flow direction. (b) Cross-channel velocity profile estimated from radial vectors in 5-m strips parallel to the estimated flow direction.

A second technique of estimating the cross-channel velocity profile was to divide the area on the river surface into strips 5 m wide, aligned parallel to the estimated flow direction as determined above. Within each 5-m strip, the along-channel velocity was estimated as the velocity which had a least-squares fit when projected on the directions of all the radial vectors falling within the 5-m strip. An example of such an estimate is shown in Fig. 5b. The sample mean and standard deviation over the 20 individual data points are shown along with the median of the 20 data points. The median tended to be more stable than the mean value, and it was used in the subsequent data processing.

Finally, a single mean velocity estimate for each hour was made by calculating the mean of the cross-channel median velocity estimates over the strips from 40 to 80 m from the radar antenna (10 to 50 m from the near bank), for which the flow generally was stable and the radar signals were strong. A time series of the mean velocity estimates for a two-week period is shown in Fig. 6, along with the river stage height data and hourly wind vectors. The river stage height data were obtained from *http://waterdata.usgs.gov/wa/nwis/uv?14243000.* The relative scales of the radar velocity and water height have been adjusted based on a least-squares fit between radar velocity and water height. The agreement between the radar velocity and water height is immediately apparent. Using the Regress function of Mathematica, a linear regression of radar velocity on water height alone yielded a model coefficient of determination R^2 of 0.926. Including the square of the water height and the along- and cross-channel wind raised the model R^2 to 0.933.

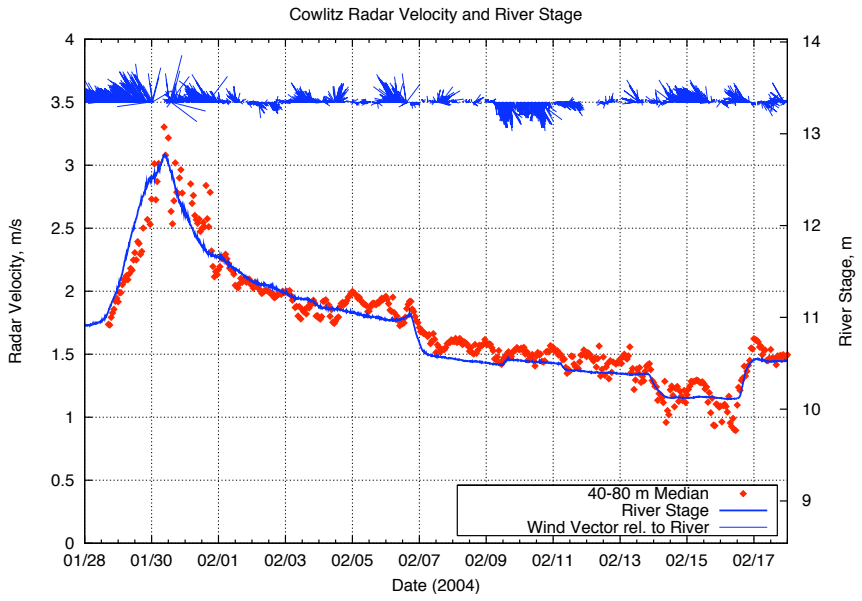

Figure 6: Time series of radar velocity (points), river stage height (solid line), and wind vectors for 28 January to 18 February 2004. Wind vectors vertically upward indicate flow upstream (opposing the water flow).

Also obvious is a roughly periodic variation in the radar velocity, on the order of 10 cm/s, which does not seem to be reflected in the height data. (Note that there are rapid jumps in the height curve, indicating that the height measurements were done with sufficient bandwidth to pass signals with periods of a few hours.) Initially it was suspected that periodic variations in wind velocity might be responsible, as the radar is sensitive to water velocity at the topmost 3 or 4 cm of the water column [*Stewart and Joy*, 1974] which is strongly coupled to the wind. Indeed, that suspicion prompted the installation of the weather station. However, from Fig. 6 there appears to be little correlation between the wind vectors and the periodic radar signal.

A Fourier time-series analysis was applied to the radar data from 2 February to 22 March, interpolating across occasional gaps of one to three hours. A plot of the resulting power spectrum is shown in Fig. 7. This figure represents a single transform, so it is noisy, but several distinct peaks

are evident, especially near 1 and 2 cycles/day, with additional peaks near 0.5 cycle/day. The peaks at 1 and 2 cycles/day suggest that some of the periodic signal in the radar velocity data may have frequencies matching tidal frequencies. Consequently, a set of tidal components consisting of the M_2, S_2, N_2, K_2, K_1, O_1, P_1, Q_1, M_4, MS_4, MF and MM terms [*Pond and Pickard*, 1989] was added to the model. Recalculating the linear regression yielded a model R^2 of 0.936. As expected from Fig. 7, the largest contributions to the model variance came from the diurnal and semi-diurnal components, but their combined contribution to the model R^2 was only 0.0025, compared to 0.926 for the linear height term. With the 87-day duration of the radar velocity time series, it was difficult to distinguish among several closely-spaced components. Nevertheless, the effect of their inclusion can be seen in Fig. 8, which shows the radar data, the prediction from height and wind terms alone, and the prediction from the full model. The inclusion of the tidal components clearly models the periodic variations in the radar velocity, although there is some residual error left. Some of the errors may be due to the omission of any energy at the three peaks near 0.5 cycle/day in Fig. 7 which do not correspond to common tidal components. Figure 8 shows a 10-day data segment, but the predicted functions were calculated based on the entire 87-day radar record, and the phase relations between the radar data and the predictions suggest a strong phase coherence over the entire record.

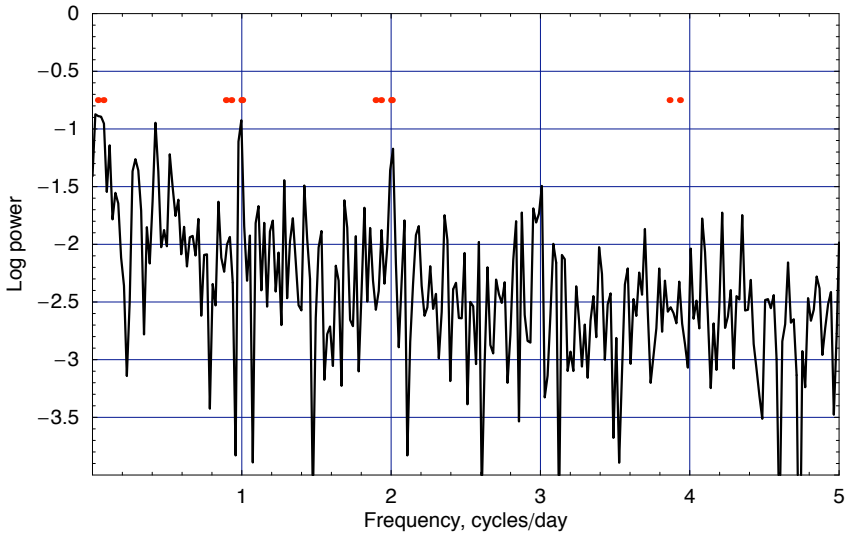

Figure 7: Power spectrum from a single Fourier transform of the radar velocity time series of Fig. 6 from 2 February to 22 March 2004. Positions of several dominant tidal frequencies are indicated by red dots.

Data Comparisons

Cross-channel velocity profiles from USGS measurements were available for two days, 22 January 2004, for which the velocity was about 1.0 m/s, and 30 January 2004, when the velocity reached about 3.5 m/s. Unfortunately, the RiverSonde was not operating on 22 January, so the records

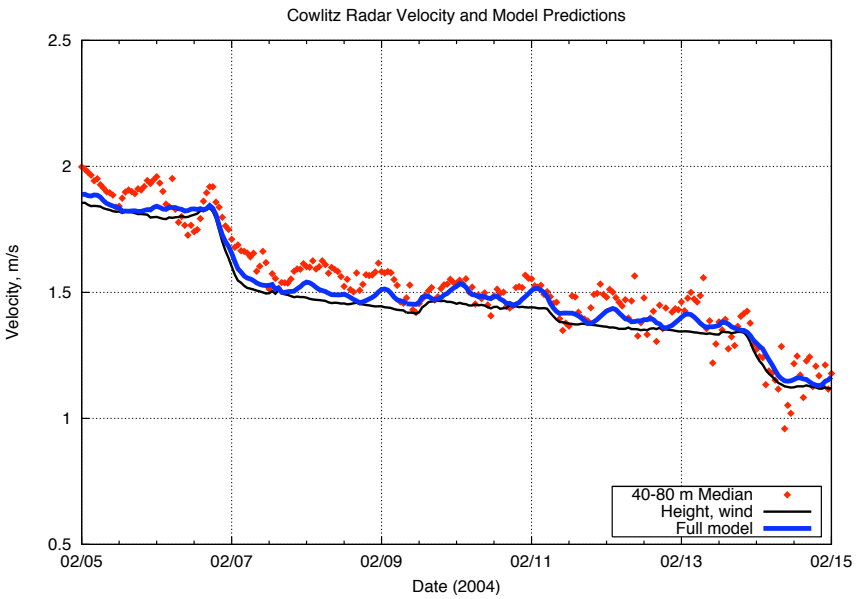

Figure 8: Comparison of a 10-day sequence of radar velocity data (red points), a model which includes only height and wind terms (thin black line), and a model which includes height, wind and tidal terms (thick blue line).

were searched for other days with similar river stage heights. On 22 January, the river stage was 33.23 ft, and on 16 February, the river stage was 33.21 ft, so that day was used for the comparison. Fig. 9 shows the USGS data taken at the bridge downstream of the radar and at the cable slightly upstream of the radar on 22 January, and the RiverSonde profiles from 16 February. The agreement between the radar and *in-situ* measurements is good for the central portion of the river, but the *in-situ* measurements fall off more quickly at both banks than the radar measurements.

Fig. 10 shows the USGS and radar measurements for 30 January 2004, when the velocity was about 2.5 m/s. Again, the agreement is good in the central portion of the river, with the USGS measurements falling off more quickly at the two edges, although the agreement is better at the near bank than in Fig. 9. There may be several reasons for the differences at the two banks. At the near side, the bank may have shadowed the water surface, as the radar was set back about 30 m from the bank. At the far bank, the radar signals were weak, with most of the available echoes coming from directions perpendicular to the direction of flow, so reliable velocity estimates were difficult to make there. In addition, the radar range cell spacing was 5 m, but with a Hamming window applied to the range processing, the effective range resolution was about 7 m. Most of the velocity falloff seen in the *in-situ* measurements occurs in the last 10 m, so the radar measurements probably did not have sufficient range resolution to see that variation. Finally, there may have been some extraneous signals in the radar hardware.

The RiverSonde velocity measurements were combined with estimates of the channel cross-section area to provide an estimate of the total discharge volume. Ground-penetrating radar (GPR) measurements of the bottom profile, made from a platform suspended on a cable across the river, were

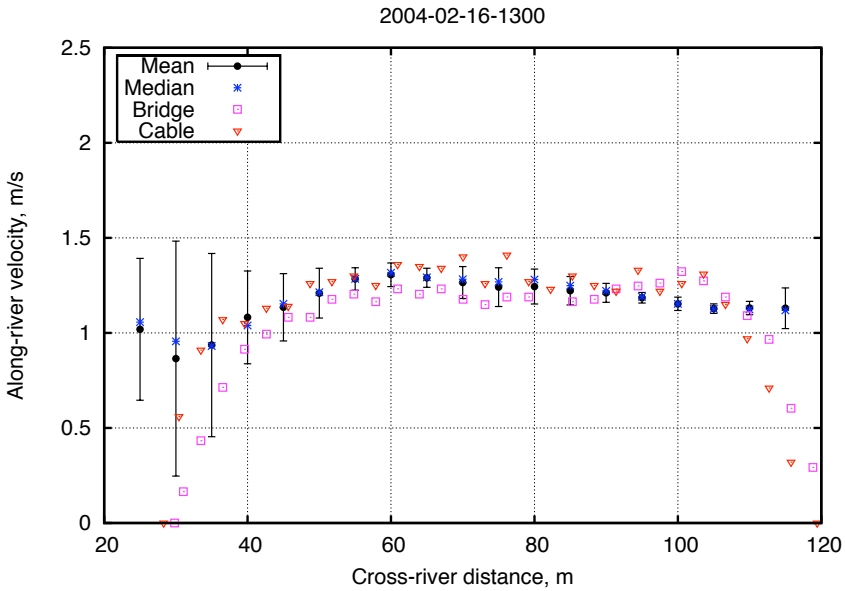

Figure 9: Cross-channel profiles from USGS measurements on 22 January 2004 and RiverSonde measurements on 16 February 2004 for very similar river stages. USGS measurements were taken at the bridge downstream of the radar and at the cable slightly upstream of the radar.

available for 30 October 2003. The reported stage height on that day was 9.68 m (31.77 ft). Since the GPR profile was available for only one day, and the stage varied from day to day, the total cross-section was estimated by assuming vertical banks at both sides above the water height at the time of the GPR measurement, and adding (or subtracting) the area of a rectangle with constant width from 30 to 118 m from the radar antenna and a height given by the difference between the hourly stage measurement and the height of 9.68 m at the time of the GPR measurement. The GPR measurement and a schematic of the estimated time-variable area are shown in Fig. 11. Both the hourly velocity and depth profiles were interpolated to 1-m intervals to simplify the integration, and the radar velocity was multiplied by the standard coefficient of 0.85 to obtain a depth-averaged velocity estimate.

The volume discharge was first computed using the stage height data provided by the USGS *in-situ* measurements. Fig. 12a shows the hourly estimates of volume discharge obtained using the RiverSonde velocity measurements and the discharge estimated by the USGS based on the rating curve for the stage height at Cowlitz. In general the agreement is quite good, with the RiverSonde estimates slightly below the rating curve, except for the high-discharge pulse on 30 January 2004, where the RiverSonde estimates were somewhat above the estimates from the rating curve. The agreement is somewhat better in the early part of the experiment than in the later period.

A linear regression of the radar-inferred discharge on the USGS estimate of discharge from the rating curve was performed for 1367 data points obtained between 27 December 2003 and 9 March 2004. The regression analysis gives $Q_r = -36.0 + 1.08 Q_u$ m^3/s, with a coefficient of determination R^2 of 0.977, where Q_r is the discharge estimated from the RiverSonde measurements and Q_u is the

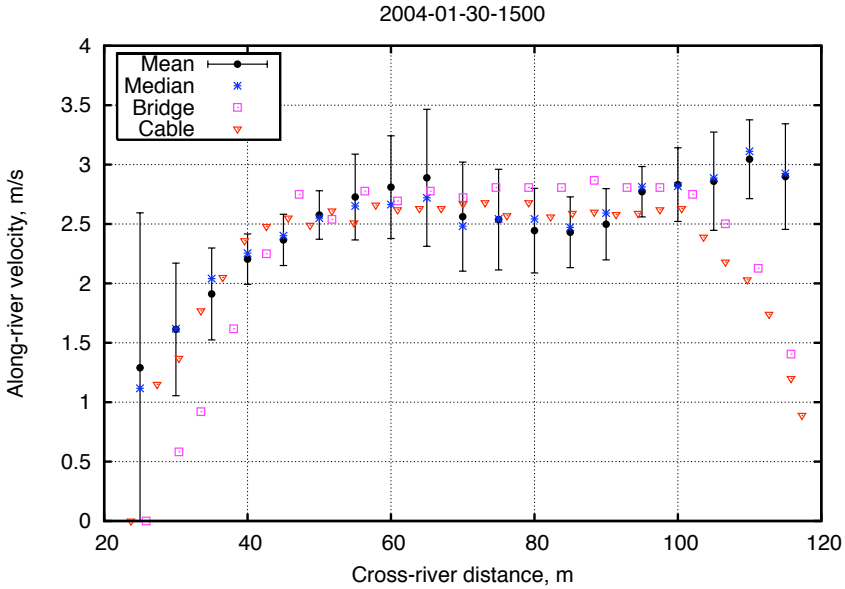

Figure 10: Cross-channel profiles from USGS and RiverSonde measurements taken on 30 January 2004. USGS measurements were taken at the bridge downstream of the radar and at the cable slightly upstream of the radar.

discharge estimated by the USGS. The RMS difference between the two estimates is 22.9 m^3/s.

For this particular site, the high correlation between velocity and stage height suggests a second procedure. The stage height was estimated from the RiverSonde velocity measurements alone, using the relation $h_r = 8.62 + 1.30v_r$, where h_r is the height (m) estimated from the RiverSonde velocity v_r (m/s). Fig. 12b shows the hourly volume discharge estimated using the RiverSonde to estimate both velocity and stage height. The estimates are quite similar to those using the *in-situ* stage height data, although a little noisier. The regression analysis gives $Q_r = -21.8 + 1.05Q_u$ m^3/s, with a coefficient of determination R^2 of 0.949, where Q_r is the discharge estimated from the RiverSonde measurements and Q_u is the discharge estimated by the USGS. The RMS difference between the two estimates using this method is 33.5 m^3/s.

The microwave system operated by the University of Washington generally was in operation at the same time as the RiverSonde. Fig. 13 (generated by Bill Plant) shows time series for both the microwave system and the RiverSonde for a period of about 108 days from 13 November 2003 to 1 March 2004. The periodic signal discussed above was evident in the data from both the microwave and RiverSonde systems. The two radar systems agreed quite well during the 108 days plotted.

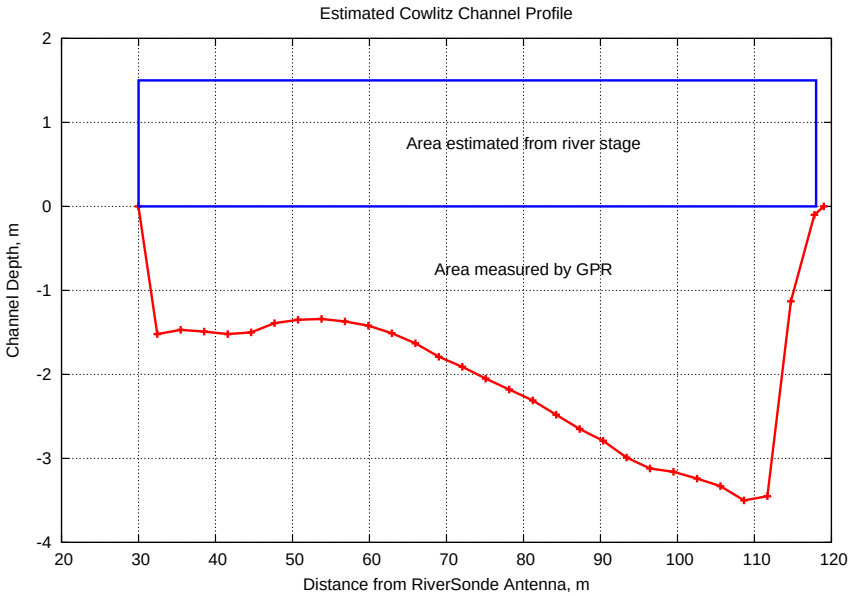

Figure 11: Bottom profile obtained using a Ground-Penetrating Radar (GPR) on 30 October 2003 (red) and area estimated from *in-situ* stage height measurements (blue) for a stage height 1.5 m above the height at the time of the GPR measurement. The top rectangular area was estimated by assuming a constant channel width and a height difference with respect to the height at the time of the GPR measurement.

Summary and Discussion

The RiverSonde system was in nearly continuous operation at Castle Rock for at least eight months from its installation on 28 October 2003 to its removal on 30 June 2004, except for about two weeks during the early part of the experiment. During the course of the experiment, the stage height varied from about 9 to 14 m, and the flow velocity varied from about 0.8 to nearly 3.5 m/s. Over that range, there was a very high correlation between RiverSonde-inferred flow velocity and measured river stage height, with an R^2 value of at least 0.93. The volume discharge using the RiverSonde velocity and the *in-situ* stage height tracked the USGS discharge with an R^2 value of nearly 0.98 and an RMS difference of 22.9 m^3/s. Replacing the *in-situ* height with the height estimated from the RiverSonde velocity resulted in a volume discharge estimate which tracked the USGS discharge with an R^2 of 0.95 and an RMS difference of 33.5 m^3/s. Note that the nearly linear relation between velocity and stage height seen at the Cowlitz site would not be expected at all sites, particularly those whose flow is dominated by tidal effects.

The influence of the wind on the estimated velocity was very small, on the order of 1 cm/s or less, but there were periodic variations on the order of 10 cm/s which have frequencies similar to the dominant diurnal and semi-diurnal tidal frequencies. Both the stage height and water velocity at the confluence of the Cowlitz and Columbia Rivers are strongly influenced by the tide, with dominant components of K_1 (23.93h) and M_2 (12.42 h), so it is not surprising to see a signature at

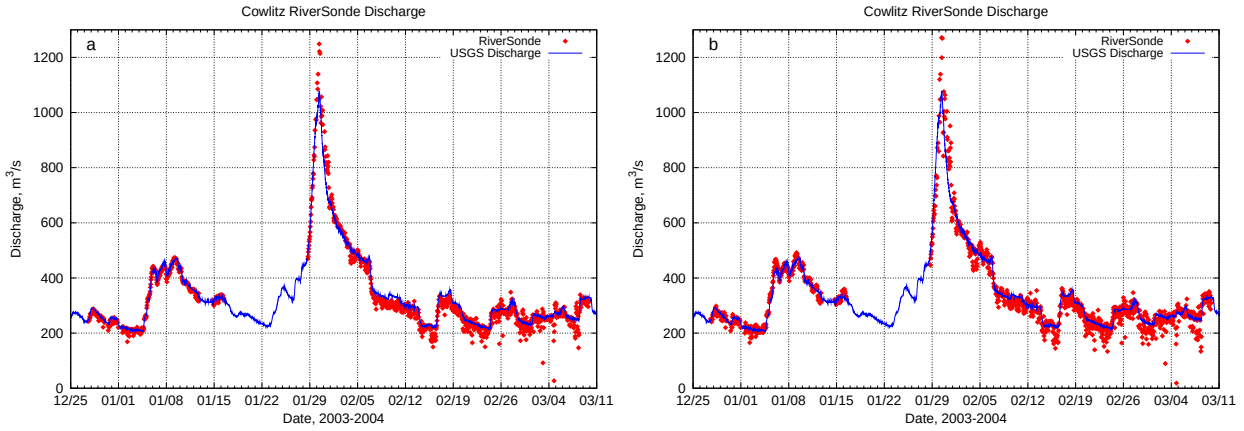

Figure 12: Estimates of volume discharge determined from the RiverSonde velocity measurements and the estimated cross-sectional area (red) and the discharge estimated by the USGS from the *in-situ* stage height measurements (blue). (a) Stage height taken from USGS *in-situ* measurements. (b) Stage height estimated from RiverSonde velocity measurements.

tidal frequencies at Castle Rock. However, this signature does not seem to be present in the Castle Rock stage height data. There also appear to be some frequency components near 0.5 cycles/day which are not obviously related to the common tidal constituents.

The RiverSonde and *in-situ* measurements showed good agreement for the available data sets. The RiverSonde system did not show the falloff in velocity at the two banks, but that might have been due to bank shadowing at the near bank and limited signal level at the far bank. The RiverSonde and microwave systems showed similar time series over several months of operation.

When the system was initially installed and throughout the winter, the foliage on the trees between the radar and the water was minimal. Throughout the spring, the leaves reappeared, and there was some concern that they might attenuate the signal somewhat. There appeared to be little degradation due to the foliage, so this does not appear to be a serious problem at 350 MHz. This is consistent with many years of use of radar frequencies in this range for foliage penetration. Nevertheless, it is possible that some of the scatter in the discharge data of Fig. 12 is related to the reappearance of foliage.

After some initial adjustment of the processing algorithms, the data processing was completely automatic, and data were available within an hour of their collection via a dial-up modem connection. All data, including the raw measurements, are archived to disks in case subsequent reprocessing is desired. The strong correlation between radar-inferred surface velocity and river stage height suggest that the RiverSonde may be attractive for routine monitoring of medium-sized rivers. The experiment should be repeated at different locations to explore any environmental influences.

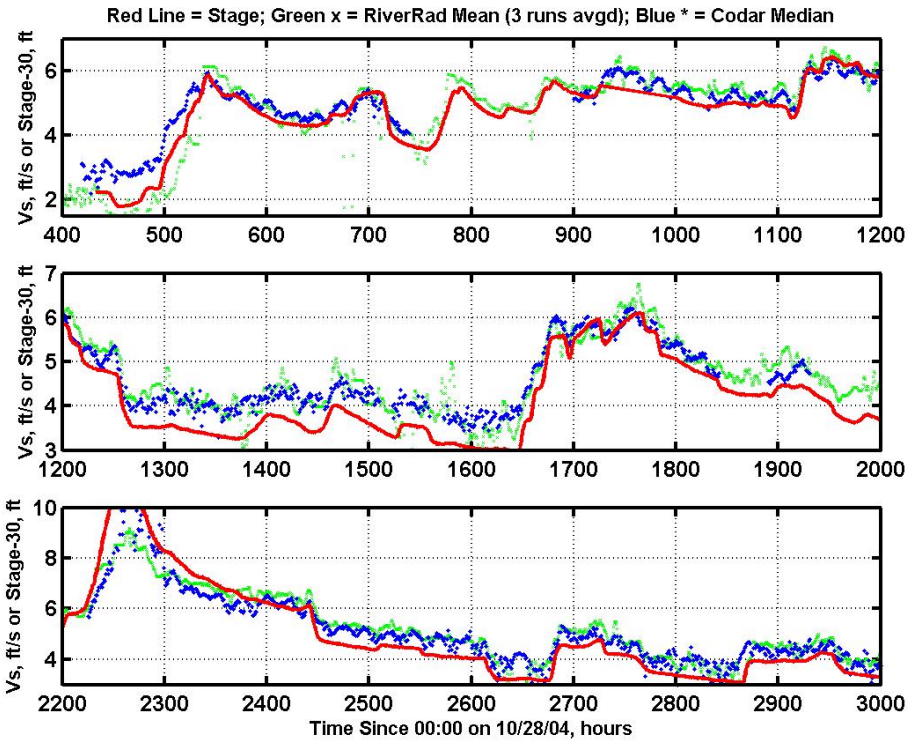

Figure 13: Time series for 108 days from the RiverSonde and microwave systems, from 13 November 2003 to 1 March 2004.

Future Work

After the RiverSonde equipment was removed from Castle Rock, it was installed at Threemile Slough in central California (between the San Joaquin and Sacramento Rivers) on 17 September 2004. In contrast to the Cowlitz River, the flow at Threemile Slough is almost completely dominated by tidal effects, with flows of roughly equal velocity in opposite directions during the tidal cycle. It is also much wider, which will test the maximum range obtainable with the system. It will be interesting to compare the results obtained there with previous results.

Acknowledgments

The authors acknowledge the support of the Hydro-21 Committee of the U. S. Geological Survey for the planning and execution of the experiment, and the city of Castle Rock, Washington for providing shelter for the equipment.

References

Barrick, D. E., Theory of HF/VHF propagation across the rough sea. Part II: Application to HF/VHF propagation above the sea, *Radio Science, 6*, 527–533, 1971.

Barrick, D. E., J. M. Headrick, R. W. Bogle, and D. D. Crombie, Sea backscatter at HF: Interpretation and utilization of the echo, *Proc. IEEE, 62*, 673–680, 1974.

Crombie, D. D., Doppler spectrum of sea echo at 13.56 mc/s, *Nature, 175*, 681–682, 1955.

Pond, S., and G. L. Pickard, *Introductory Dynamical Oceanography*, second ed., Permagon Press, 1989.

Schmidt, R. O., Multiple emitter location and signal parameter estimation, *IEEE Trans. on Antennas and Propagation, AP-34*, 276–280, 1986.

Stewart, R. H., and J. W. Joy, HF radio measurement of surface currents, *Deep-Sea Research, 21*, 1039–1049, 1974.

Teague, C., D. Barrick, and P. Lilleboe, Vernalis May 2002: Preliminary Report, *Tech. rep.*, CODAR Ocean Systems, Ltd., 2002.

Teague, C. C., D. E. Barrick, P. Lilleboe, and R. T. Cheng, Canal and river tests of a RiverSonde streamflow measurement system, in *IEEE 2001 International Geoscience and Remote Sensing Symposium Proceedings*, pp. 1288–1290, IEEE, New York, 2001, IGARSS'01, Sydney, Australia.

Teague, C. C., D. E. Barrick, P. M. Lilleboe, and R. T. Cheng, Initial river test of a monostatic riversonde streamflow measurement system, in *Proc. of the IEEE/OES Seventh Working Conference on Current Measurement Technology*, edited by J. A. Rizoli, pp. 46–50, IEEE, New York, 2003.